AD-A244 083

MENTATION PAGE

Form Approved
OMB No. 0704-0188

estimates to average 1 hour per response, including the time for reviewing instructions, searching existing data sources, g and reviewing the collection of information. Send comments regarding this burden estimate or any other aspect of this g this burden, to Washington Headquarters Services, Directorate for Information Operations and Reports, 1215 Jefferson to the Office of Management and Budget, Paperwork Reduction Project (0704-0188), Washington, DC 20503.

2. REPORT DATE

3. REPORT TYPE AND DATES COVERED
ANNUAL 15 Nov 90 To 14 Nov 91

4. TITLE AND SUBTITLE
PREDICTION OF GLOBAL CLOUD COVER WITH A VERY HIGH RESOLUTION GLOBAL SPECTRAL MODEL

5. FUNDING NUMBERS
GR - AFOSR-91-0023
PE - 61102F
PR - 2310
TA - CS

6. AUTHOR(S)
Dr T.N. Krishnamurti

7. PERFORMING ORGANIZATION NAME(S) AND ADDRESS(ES)
Florida State University
Department of Meteorology, B-161
Tallahassee, FL 32306-3034

8. PERFORMING ORGANIZATION REPORT NUMBER
AFOSR-TR- 91 0994

9. SPONSORING/MONITORING AGENCY NAME(S) AND ADDRESS(ES)
James G. Stobie, Lt Col, USAF
AFOSR/NL
Building 410
Bolling AFB DC 20332-6448

DTIC
ELECTE
DEC 26 1991
S C D

10. SPONSORING/MONITORING AGENCY REPORT NUMBER

11. SUPPLEMENTARY NOTES

12a. DISTRIBUTION/AVAILABILITY STATEMENT
Approved for public release;
distribution unlimited

12b. DISTRIBUTION CODE

13. ABSTRACT (Maximum 200 words)

We have completed two papers in relation to the objectives of this grant. 1. Inclusion of anvil rain in cumulus parameterization scheme. 2. Prediction of fractional cloud cover and the outgoing long wave radiation in a global model. These two papers are closely interrelated in that the first paper addresses a substantial improvement for our definition of tropical cloud cover, while the second paper addresses its application over the global belt via 4 to 6 day long prediction experiments.

91-18912

14. SUBJECT TERMS

15. NUMBER OF PAGES

16. PRICE CODE

17. SECURITY CLASSIFICATION OF REPORT	18. SECURITY CLASSIFICATION OF THIS PAGE	19. SECURITY CLASSIFICATION OF ABSTRACT	20. LIMITATION OF ABSTRACT
UNCLASSIFIED	UNCLASSIFIED	UNCLASSIFIED	UNLIMITED

Accession For
NTIS GRA&I
DTIC TAB
Unannounced
Justification
Distribution/
Availability Codes
Avail and/or
Special
A-1

Non–competing, Continuation Technical Proposal
Year 2 – 11/15/91 – 11/14/92

PROJECT TITLE: Prediction of Global Cloud Cover with a Very High Resolution Global Spectral Model
P.I.: Dr. T.N. Krishnamurti
GRANT NO.: AFOSR–91–0023
DURATION OF GRANT: 11/15/90 – 11/14/93
UNIVERSITY ADDRESS: Florida State University
Department of Meteorology, B–161
Tallahassee, FL 32306–3034

DTIC COPY INSPECTED 6

We have completed two papers in relation to the objectives of this grant.

1. Inclusion of anvil rain in cumulus parameterization scheme.
2. Prediction of fractional cloud cover and the outgoing long wave radiation in a global model.

These two papers are closely interrelated in that the first paper addresses a substantial improvement for our definition of tropical cloud cover, while the second paper addresses its application over the global belt via 4 to 6 day long prediction experiments.

In the first paper we propose a method for improving the definition of tropical anvil clouds and the accounting of anvil rain within an improved cumulus parameterization scheme. This method is designed to improve the field of the net outgoing long wave radiation and thus the overall global tropical cloud cover.

The motivation for this study came from two recent studies on the improvement of the initialization and prediction of the outgoing longwave radiation (OLR), Weiner (1990) and Krishnamurti et al. (1991). Fig. (1a,b,c) from their studies shows a comparison of a satellite based measure of the OLR (fig. 1a), an OLR field based on a radiation algorithm of a global model using ECMWF analysis of the humidity field (fig. 1b) and an OLR field based on the same radiation algorithm of the global model when the humidity analysis was restructured to provide a closer match of the observed and the initialized OLR (fig. 1c). A bisection method was used to define a single parameter structure function of the humidity variable in the upper troposphere which minimized the difference between the observed and the computed OLR (fig. 1a and 1c). In comparison to a control run initialization (fig. 1b) the modified humidity provided a much improved definition of the OLR (fig. 1c).

It was furthermore noted by Weiner (1990) that this improvement in the OLR initialization resulted in an improved forecast of the OLR when it was compared to the

15 NOV 1991

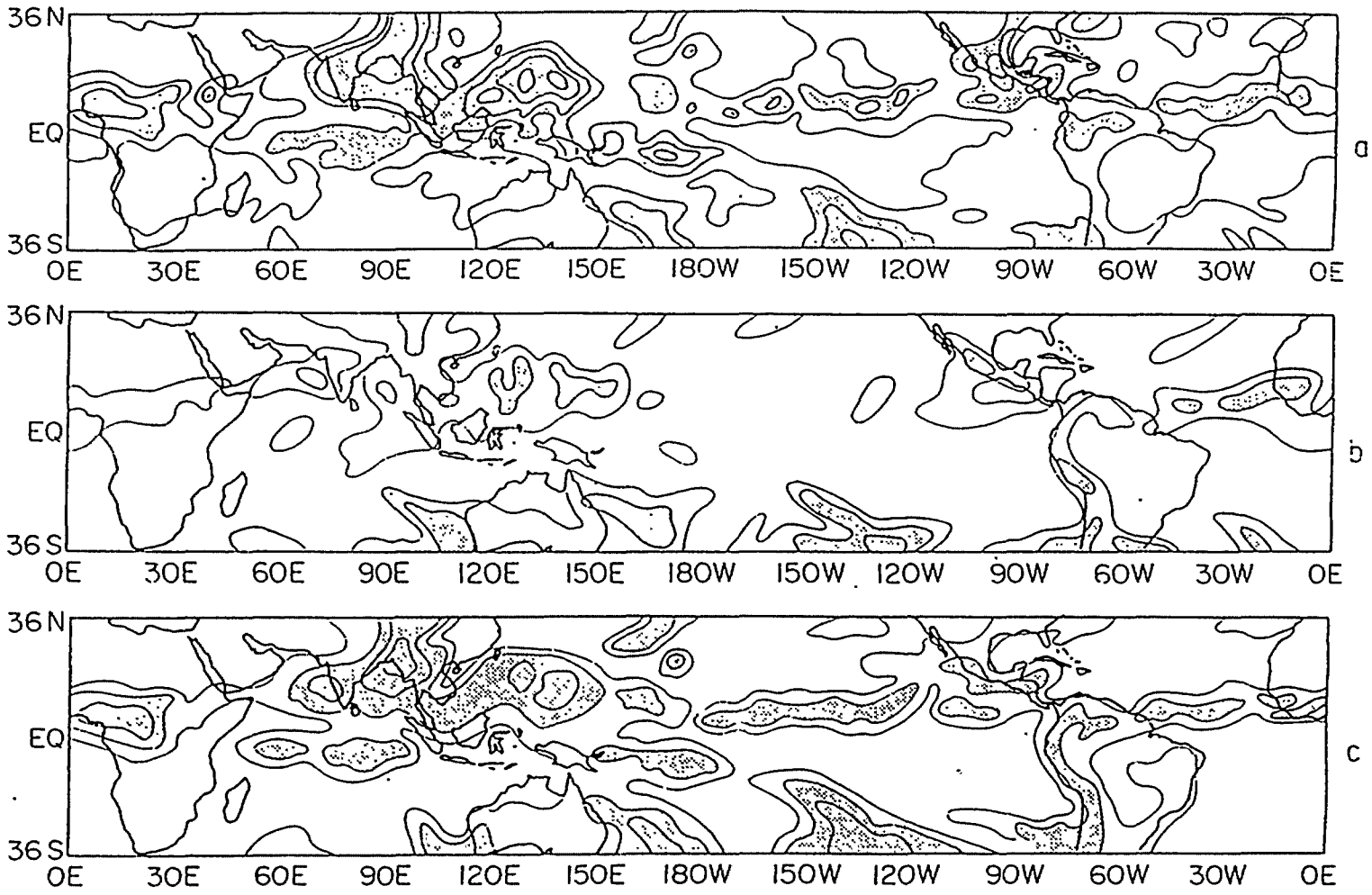

Fig. 1 Field of the initial outgoing long-wave radiation, (27 July 1979) (W/m^2). Interval of analysis 40 W/m^2, shaded area denotes values less than 240 W/m^2. (a) Based on polar orbiting satellite data sets. (b) Based on a control experiment forecast at a resolution T106. (c) Based on Newtonian relaxation experiment at a resolution T106.

forecasts made for the control case. Weiner (1990) study went one step further in stating that for the medium range time scale, i.e. 5 to 10 days, an OLR based rainfall algorithm (which is not a part of the model) might in fact provide a better estimate of the predicted rain when it is compared with the model based rainfall algorithm – i.e. its cumulus parameterization and the large scale condensation. Weiner showed example of this where indeed the skill in the forecast of OLR (starting from the improved OLR initialization, fig. 1c) provided a better inferred rain from the predicted OLR as compared to what the model's rainfall forecast provided. In these experiments a global spectral model, outlined by Krishnamurti et al.(1990), was integrated at a resolution T42.

The higher skill in OLR forecasts evidently came from the improvement of the humidity analysis of the upper troposphere. The rainfall algorithms from the OLR are based on the studies of Janowiak and Arkin (1991) and Krishnamurti et al.(1983).

Thus it appears that useful information content resides in the OLR based rain (which is not a part of the model's rain forecast) and that could perhaps be passed on to the models rainfall mechanisms. That was a motivation for the present study.

The second study is on the evaluation of the forecast skill for the global fractional clouds by this proposition. Basically this includes a comparison of results of several experiments which are:

i) A control run where the cumulus parameterization (Krishnamurti et al.(1983) does not include the provision for anvil clouds.

ii) A modified cumulus parameterization where the effects of cloud anvil are included and

iii) A repeat of experiment (ii) where the global conservation of specific humidity q and q^2 are imposed rigorously.

The results of these experiments have been rather striking. A few examples of the predicted cloud cover at day 5 from the three experiments are included in the following pages. These show that the combination of the parameterization of the anvils and the conservation of moisture (and its variance) has indeed produced a marked improvement in the initialization and prediction of global tropical cloud cover.

The few sample diagrams shown from the second study exhibits a marked improvement in the prediction of fractional cloud cover and the field of net outgoing long wave radiation. Here we show a comparison of the results from the following three experiments:

i) A control experiment, which is based on a recent version of the FSU global spectral model, Krishnamurti et al.(1989).

ii) An experiment where the improved cumulus parameterization, including the prescription of the anvil rain is used.

iii) An experiment where in addition to ii) above we have imposed a constraint restoration for the global mean specific humidity and the global mean square specific humidity on sigma surfaces.

The sequence of charts for day 5 of a forecast are presented here:

Figure 2 (a,b,c) Fractional low clouds, panel a shows control; panel b shows the results for the parameterization of anvil rain and panel c shows the results that also includes constraint restoration.

Figure 3 (a,b,c) shows the same as above for the fractional high clouds.

Figure 4 (a,b) shows the fractional low and high clouds observed.

<u>Proposed work in the second year:</u>

1. Graduate student Peter Broll expects to complete his masters thesis on this topic.
2. We propose to go further in resolution, ie. T106 for the global model and include physical initialization to improve the initial global cloud cover and its impact on 5 to 10 day forecasts.
3. We propose to work on a case that will be provided to us by Global Weather Central (Offutt) for comparison of model products with these Offutt observations.

Figure 2 a) Fractional low cloud, control expt. T42 day 5 forecast.
b) Same for anvil rain parameterization.
c) Same for anvil rain plus constraint restoration.

Figure 3 a) Fractional high cloud, control expt. T42 day 5 forecast.
b) Same for anvil rain parameterization.
c) Same for anvil rain plus constraint restoration.

Figure 4 a) Fractional low clouds observed.
b) Fractional high clouds observed.

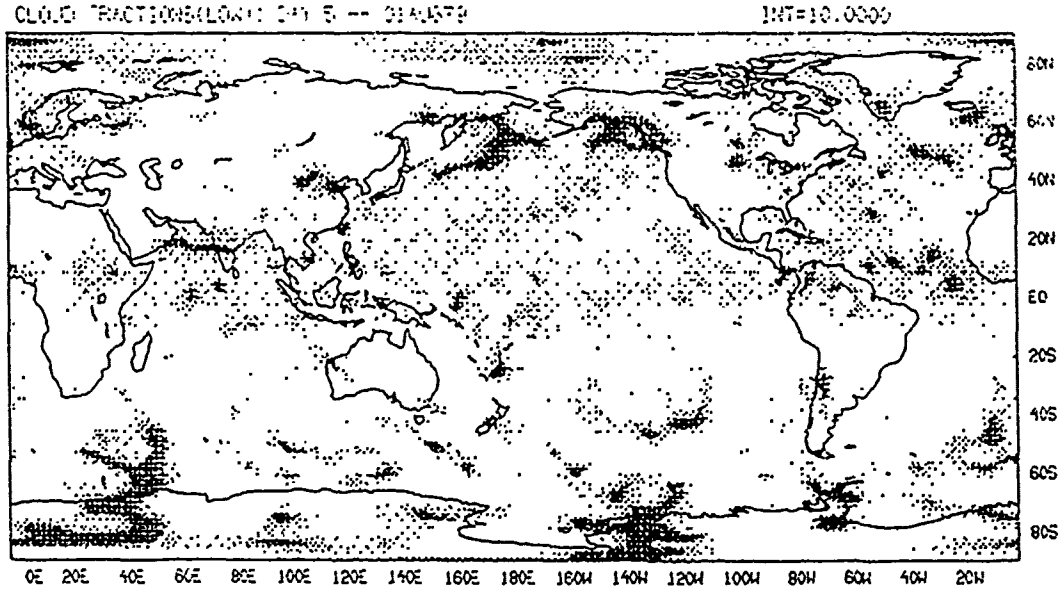
INT=10.0000
80N
60N
40N
20N
EQ
20S
40S
60S
80S
0E 20E 40E 60E 80E 100E 120E 140E 160E 180E 160W 140W 120W 100W 80W 60W 40W 20W

(a)

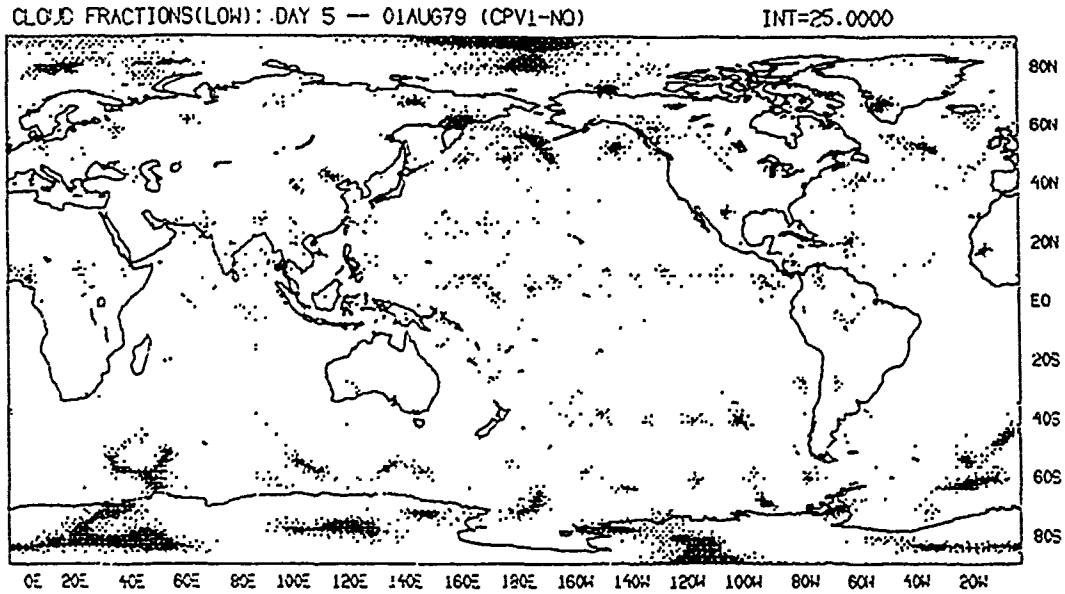
CLOUD FRACTIONS(LOW): DAY 5 -- 01AUG79 (CPV1-NO)
INT=25.0000
80N
60N
40N
20N
EQ
20S
40S
60S
80S
0E 20E 40E 60E 80E 100E 120E 140E 160E 180E 160W 140W 120W 100W 80W 60W 40W 20W

(b)

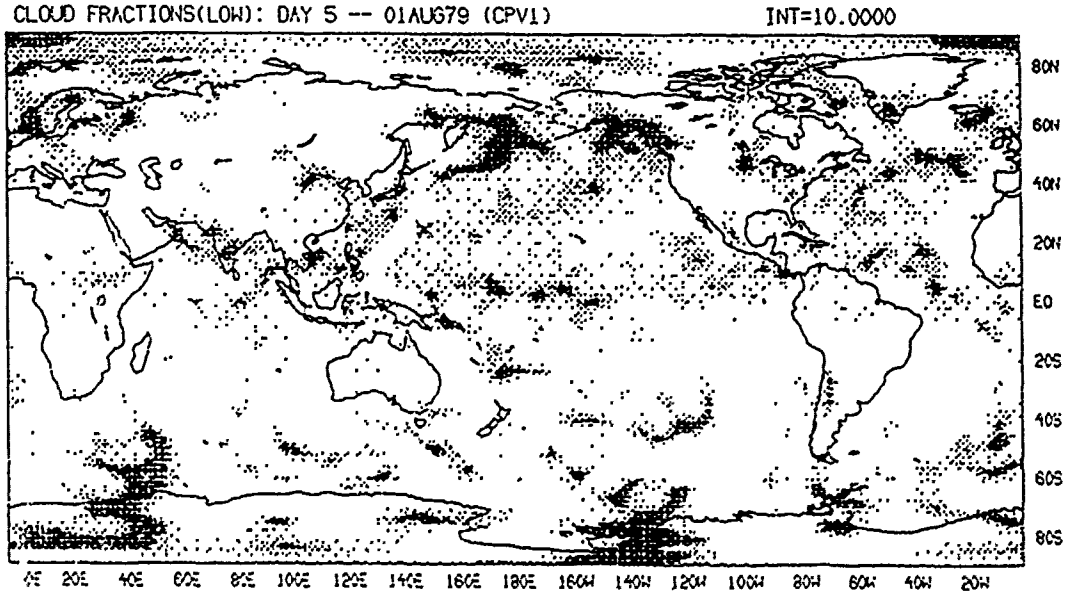
CLOUD FRACTIONS(LOW): DAY 5 -- 01AUG79 (CPV1)
INT=10.0000
80N
60N
40N
20N
EQ
20S
40S
60S
80S
0E 20E 40E 60E 80E 100E 120E 140E 160E 180E 160W 140W 120W 100W 80W 60W 40W 20W

(c)

FIG 2

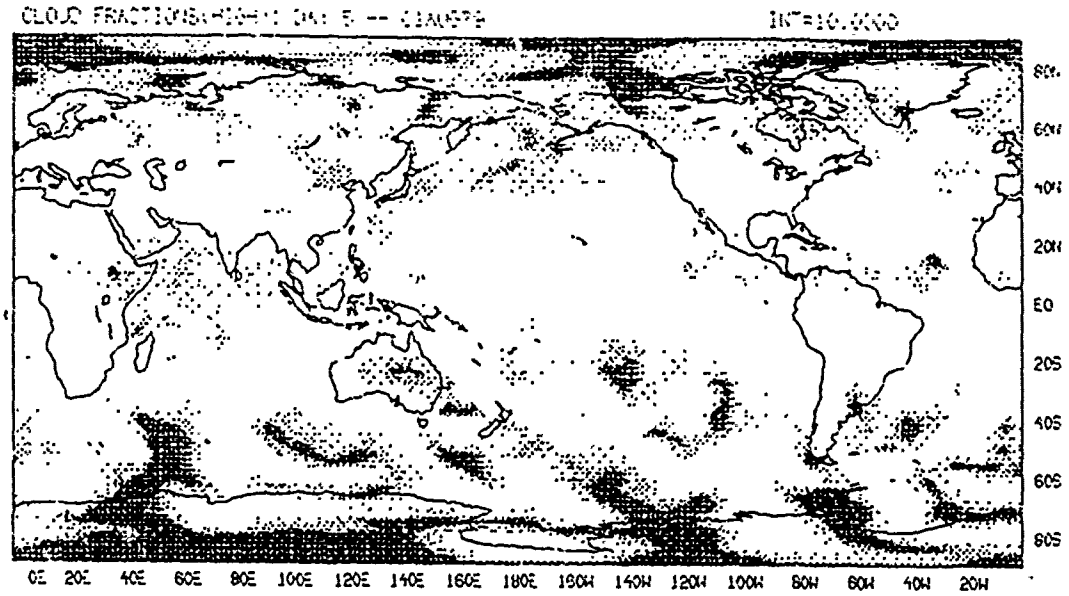
INT=10.0000
80N
60N
40N
20N
EQ
20S
40S
60S
80S
0E 20E 40E 60E 80E 100E 120E 140E 160E 180E 160W 140W 120W 100W 80W 60W 40W 20W

(a)

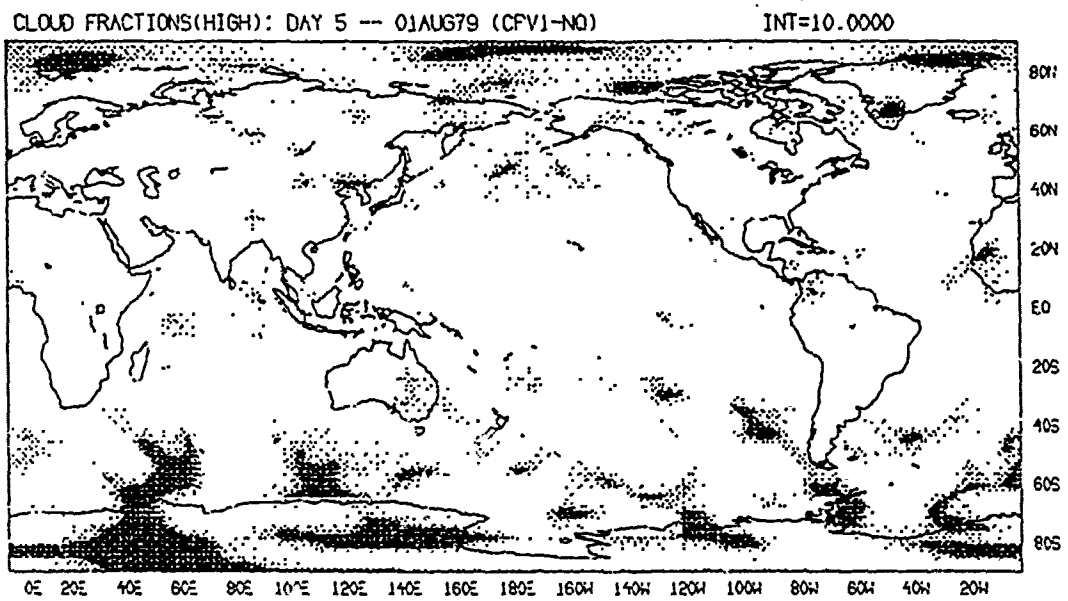
CLOUD FRACTIONS(HIGH): DAY 5 -- 01AUG79 (CPV1-NO)
INT=10.0000
80N
60N
40N
20N
EQ
20S
40S
60S
80S
0E 20E 40E 60E 80E 100E 120E 140E 160E 180E 160W 140W 120W 100W 80W 60W 40W 20W

(b)

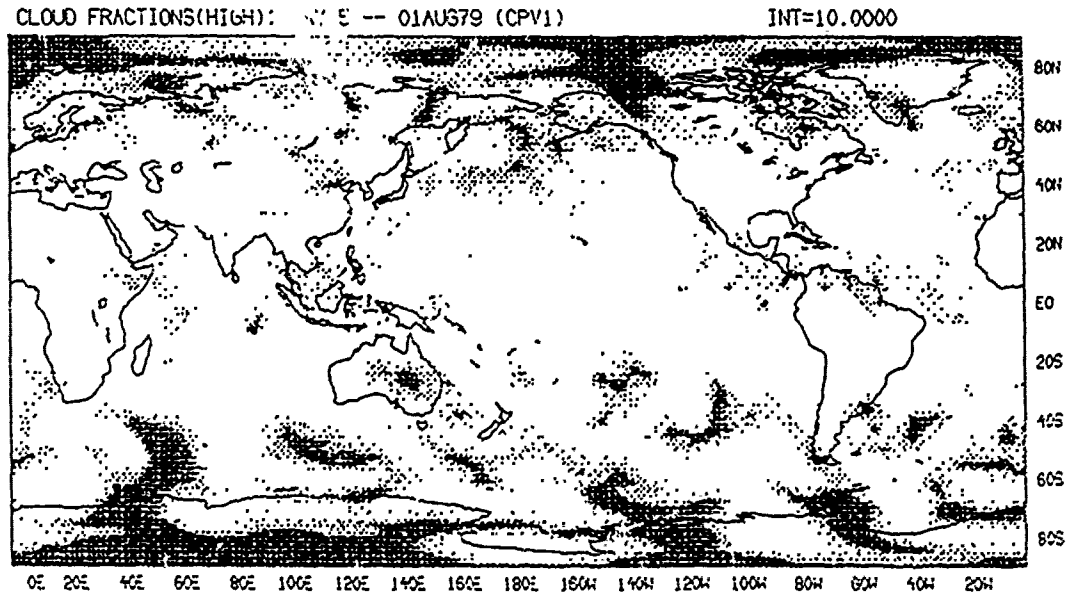
CLOUD FRACTIONS(HIGH):
-- 01AUG79 (CPV1)
INT=10.0000
80N
60N
40N
20N
EQ
20S
40S
60S
80S
0E 20E 40E 60E 80E 100E 120E 140E 160E 180E 160W 140W 120W 100W 80W 60W 40W 20W

(c)

FIG 3

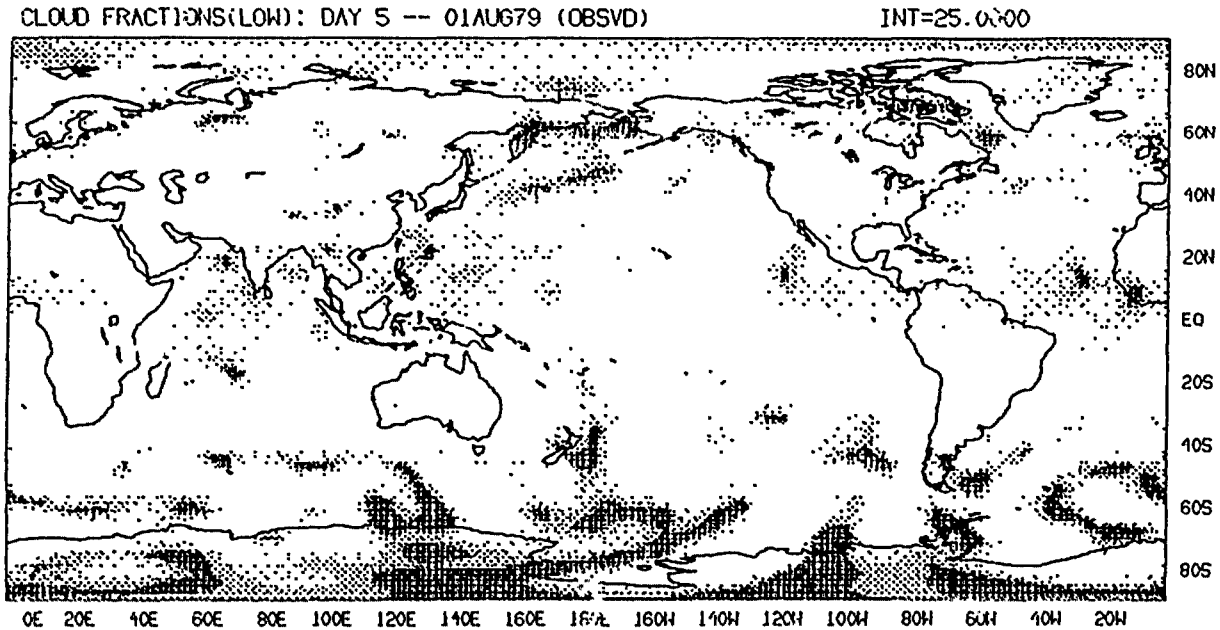
CLOUD FRACTIONS(LOW): DAY 5 -- 01AUG79 (OBSVD)
INT=25.0000
80N
60N
40N
20N
EQ
20S
40S
60S
80S
0E 20E 40E 60E 80E 100E 120E 140E 160E 180E 160W 140W 120W 100W 80W 60W 40W 20W

(a)

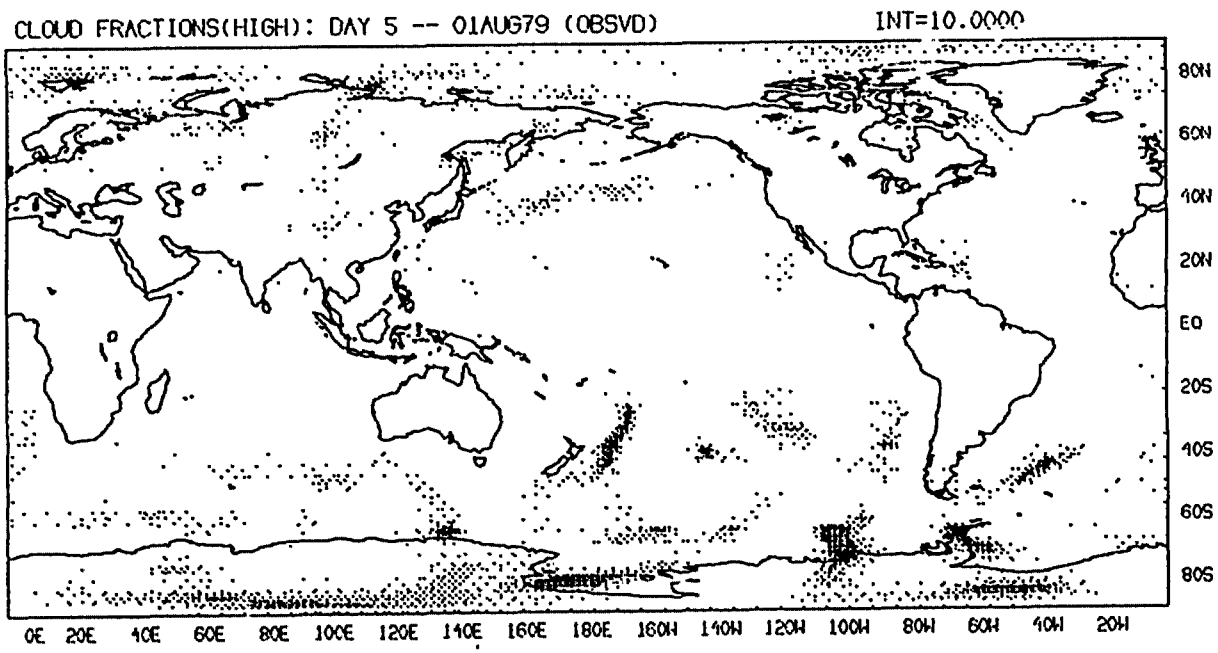
CLOUD FRACTIONS(HIGH): DAY 5 -- 01AUG79 (OBSVD)
INT=10.0000
80N
60N
40N
20N
EQ
20S
40S
60S
80S
0E 20E 40E 60E 80E 100E 120E 140E 160E 180E 160W 140W 120W 100W 80W 60W 40W 20W

(b)

FIG 4

INCLUSION OF ANVIL RAIN IN A CUMULUS PARAMETERIZATION SCHEME

MICKEY WAI
T.N. KRISHNAMURTI

FLORIDA STATE UNIVERSITY
DEPARTMENT OF METEOROLOGY
TALLAHASSEE, FLORIDA 32306–3034

1. INTRODUCTION

The skill of Numerical Weather Prediction (NWP) of atmospheric circulations has been continuously improved while the trend in precipitation forecast skill has only slightly improved. The improvement in precipitation forecasting depends heavily on refining the model's spatial and temporal resolution and the ability to model the precipitation processes. These precipitation processes generally include moisture flux and lifting, cloud microphysical processes, and the dynamics and distribution of droplets falling to the ground as precipitation. Furthermore, these precipitation processes must include parameters for estimating drizzle, rain, freezing rain, snow and hail. To model all these processes in NWP model requires a full mathematical description of these processes, particularly the growth of water drops and ice crystals. Such microphysical processes cannot be explicitly represented because of their scale and the corresponding computational requirement, they must be parameterized. Therefore, their net effects are parameterized in NWP models. How much complexity is required in parameterizing the precipitating processes is an important research topic.

The precipitation forecast in NWP models is commonly done via one of several types of the cumulus parameterization schemes: Kuo (1974), and Arakawa–Schubert (1974), Betts and Miller (1986) and others. In the first of these the cumulus convection occurs throughout layers which are conditional unstable, given a net moisture supply due to large–scale convergence or turbulent processes. The cloud is then assumed to dissipate each time step by mixing with the environmental air at each level, giving a heating and moistening at each level. This produces a gain of energy in the column as a whole which corresponds to the latent heat of the moisture convergence. The heating at each level is the consequence of condensation. The rainfall rate is then given by the vertical integration of the heating ratios at each level. This Kuo type cumulus parameterization and rainfall rate has been improved by including mesoscale moisture convergence and moistening. These are parameterized through regressing the normalized rainfall rate and moistening rate against the vertically integrated vertical velocity and the vorticity at 700 mb (Krishnamurti et al., 1983a). More recently, Krishnamurti

and Bedi (1988) recognized that the regression coefficients vary spatially; they therefore recalculated the regression equations and obtained a global set of coefficients for the mesoscale moisture convergence and moistening.

We had noted that the current cumulus parameterization does not account for anvil rain from large tropical convective systems. Tropical rain is partioned between the convective and nonconvective components. A large proportion of the latter falls from Anvils. The fraction of the total rain from Anvils can be anywhere between 10 to 40% depending on the intensity of tropical weather systems. In a simple easterly wave that is around 10% of the total rain, but it can be as large as 40% in a hurricane where a large number the number of cumulonimbus Anvils are known to cover a substantial area around the rainbands. The proposed extension of the cumulus parameterization include parameters that are functions of OLR, we perceive this as a way to include the anvil rain contributions.

The Arakawa–Schubert parameterization is achieved by parameterizing the effect of the cumulus convection on the large–scale variables by modeling the dynamics of the sub grid scale cloud ensemble (Arakawa and Schubert, 1974). The parameterization is incorporating three conditions. The first condition is to determine how the large–scale environment destablizes the convection, and in turn how the convection stabilizes the large–scale environment. This is know as the quasi–equilibrium condition. The second condition is to determine how the convection modifies its large–scale environment. In this case, the latent heating inside the cloud maintains the vertical mass flux of clouds. The third condition is to determine the thermodynamical property of clouds. Both of the above schemes seem to be supported by observational data, and it is presently impossible to give preference for one against the other (Tiedtke, 1989). Different forms of these two cumulus parameterization schemes have been tested in several cases of severe mid–latitude convective storms (see Grell et al., 1991 for review). In the present study, we address further the improvement of the Kuo–type cumulus parameterization scheme and assess the improvement via short–to–medium range forecast in the tropical precipitation. The Kuo–type cumulus parameterization and

rainfall rate scheme has been an on going research area using FSU regional and global models. Furthermore, the existing cumulus parameterization scheme is more easily to be modified and adapted into the FSU Global Spectral Model.

2. DETERMINATION OF MULTIPLE REGRESSION COEFFICIENTS

The normalized rainfall rate and moistening rates are currently expressed as a function of pairs of vertically integrated vertical velocity and 700 mb relative vorticity values. Theoretically, the two water substances can be expressed as functions of known quantities produced by the NWP model. To identify the optimum combination of these variables requires either unique physical insight on the precipitation processes in weather systems or a carefully designed experiment. Accumulated experimental evidence has shown that the outgoing longwave radiation provides a reasonable estimate of the precipitation rate (Janowiak and Arkin, 1991; Wu, 1991). Following what we have stated in the opening remarks of the paper we propose to extend the regression relations by including three additional variables associated with outgoing longwave radiation in determining the rainfall rate and moistening rate. A pair of multiple regression equations were developed; they related the vertically integrated vertical velocity, 700 mb relative vorticity, outgoing longwave radiation (OLR), the local time rate change OLR, and the horizontal Laplacian of OLR as follows:

$$\frac{M}{T_L} = q_1\zeta + b_1\overline{w} + c_1\,\mathrm{OLR} + d_1\frac{\partial}{\partial t}\mathrm{OLR} + \ell_1\nabla^2\,\mathrm{OLR} + f_1$$

$$\frac{R}{T_L} = q_2\zeta + b_2\overline{w} + c_1\,\mathrm{OLR} + d_1\frac{\partial}{\partial t}\mathrm{OLR} + \ell_1\nabla^2\,\mathrm{OLR}$$

The six coefficients of this pair of multiple regression equations are computed from the observations from the GATE A/B–scale array of ships. We obtained six time series of omega bar, 700 mb vorticity, OLR, the local time rate change of OLR, the Laplacian of OLR, and the

rainfall rate at every 6 hours. We compute two sets of coefficients: (1) excluding three OLR variables and (2) including three OLR variables. The two sets of coefficients are given in table 1. The computed rainfall rates with these two sets of coefficients along with the observed rainfall rates are shown in fig. 1. The root mean square (RMS) errors for case 1 and case 2 are 0.39 and 0.36 respectively. By including the three OLR variables in the regression equations, the RMS error has been reduced by 8%.

3. RAINFALL FORECASTS FOR 1979 TROPICAL MONSOONS

Next we forecast the tropical precipitation by incorporating this scheme of extended cumulus parameterization and rainfall rate into an FSU Global Spectral Model with a 42 wave, triangular truncation. A full description of the FSU T42 GSM can be found in Krishnamurti et al. (1990). Here only a brief summary is given. The model carries six equations in the spectral form for vorticity, divergence, thermodynamics, continuity, hydrostatics, and moisture. The vertical discretization of the FSU GSM is staggered. The variables defined on the sigma levels are vorticity, divergence, and geopotential while the temperature and moisture are placed at the intermediate levels. The model physics processes include shortwave radiation parameterization and is based on the scheme of the USLA/GLAS GSM as described by Davies (1982) and Harshvardan et al. (1987). The longwave radiation is parameterized according to the methods described by Harshvardan and Corsetti (1980). Processes of horizontal diffusion follow the method developed by MacVean (1983), and the vertical diffusion is calculated with K–theory. The shallow convection is based on the technique by Tiedtke (1989). Deep cumulus convection and large–scale condensation are based on the methods by Krishnamurti et al. (1983a). Surface fluxes are computed from similarity theory (Businger et al., 1971) and modified by Louis (1979) for NWP application.

We perform two six–day precipitation forecasts starting with data at 12Z, 27 July 1979 from FGGE IIIb data set. We define the forecast that excludes the three OLR variables in the multiple regression equations as a control experiment. The forecast that includes all three

OLR variables in the multiple regression equations is labelled as the 'OLR model' forecast. The daily accumulated precipitation from the control and the forecasts 'OLR model' forecasts are compared with the daily precipitation from the Atlas of Krishnamurti et al. (1983b). These observed data sets were obtained by assimilating the raingauge data into satellite observations. Satellite OLR observations were used to create a first–guess field of large–scale precipitation. then a Cressman analysis was then performed using the raingauge data. These analyses are not intended to be an absolute measure of precipitation, but rather it is used as a general frame of reference when comparing with the numerical forecast. The observed daily accumulated rainfall from 28 July to 1 August are shown in Fig. 2. The daily accumulated precipitation from the control and the new forecasts are shown in Fig. 3 and 4. Comparing the daily accumulated rainfall rate from figs. 2 to 4, the new forecast shows improvement in the precipitation forecast along the east coast of India, and over the region of Thailand and Vietnam for the first three days. Furthermore, the forecast also tends to capture a large area of precipitation over the Arabian Ocean and the double, local maximum precipitation in the Western Pacific tropical ocean. To assess the improved forecast quantitatively, we have computed the RMS errors for the daily accumulated precipitation and for the location of precipitation from the two forecasts. Again we take the data set produced by Krishnamurti et al. (1983b) as observations. For these, we select three sectors: (1) India bounded by 0°N to 22°N and 62°E to 80°E; (2) Burma bounded by 0°N to 22°N and 95°E to 110°E, and (3) Western Pacific bounded by 0°N to 22°N and 110°E to 150°E. The RMS errors for these three sectors from the two forecasts are given in Tables 2 and 3. In sector one, the new forecast shows that the RMS error for the accumulated daily precipitation decreased from 21.8 mm on day 1 to 14.4 mm on day 3. From day 3 onwards, the RMS error increased to 37.0 mm on day 5. However, the controlled forecast shows that the RMS error oscillates having two peak on days 2 and 4 and maintaining a value of 25 mm. Thus it does not show a distinctive decrease with time. The RMS error for the location in the new forecast increased slightly form 0.45 on day 1 to 0.54 on day 3, and increased to 0.70 on day 5. During the first three days, the RMS

error remains smaller in the forecast than those in the control forecast. In sector 2, the daily accumulated precipitation from both forecasts shows oscillation and does not show a distinctive decrease with time. However, the RMS error for the location from the new forecast decreased from 0.61 on day 1 to 0.54 on day 3, it then increased back to 0.69 on day 5. In contrast, the RMS error for this location in the controlled forecast remained at 0.59 for the first three days before it dropped slightly to 0.56 on day 5. In sector three, the areas are mostly over the ocean where there are not raingauge data to be assimilated into the precipitation estimated from satellite data. We only compare the RMS for the location from the two forecasts. The RMS error from the new forecast decreased from 0.62 on day 1 to 0.54 on day 3 before it increased to 0.72 on day 5, while the RMS error from the controlled forecast remained around 0.7 for the five days. The RMS error analyses indicated that the precipitation and location show a three day forecast improvement, except for the daily accumulation rainfall rate in sector two. The poor forecast is probably due to the coarse resolution which cannot capture the moisture supply. Overall, the RMS errors were smaller in the new forecast as compared to the control forecast.

4. SENSITIVITY OF RAINFALL FORECAST WITH SELECTIONS OF OLR

The sensitivity of the selection of these three OLR variables to the precipitation forecast is discussed here. Practically, it is desirable to include the least numbers of variables in the regression equations, yet maintain the same performance as if including all variables. The least number of variables in the regression equations would take less computational time and require less bookkeeping of these variables; this is particularly true of the local time rate change of the OLR because it is presently calculated every three hours. We perform three additional experiments: (1) including OLR; (2) including OLR and the time rate change of OLR; and (3) including OLR and the Laplacian of the OLR. Similar to the previous two forecasts, we calculate the RMS errors for the daily accumulated precipitation and the location of the precipitation forecast for the same three sectors in section 3. The RMS errors are

summarized in tables 4 to 6. Two forecasts, that which includes OLR alone, and combined OLR and the time rate change of OLR, give relatively large RMS errors when compared with those from the new forecast and show that the RMS errors increase with time. However, forecasts, that just include OLR and the Laplacian of OLR, show a similar three–day improvement in the daily accumulated rainfall in the India and the Western Pacific sectors and the location in the East Asia and the Western Pacific sectors. Although the RMS error in the location forecast increases with time in the India sector, the values of the RMS are still smaller than those in the controlled forecast. Generally, the values of RMS errors are only slightly larger but comparable to those from the three variables forecast. Therefore, it is concluded that only OLR and the Laplacian of the OLR need to be used in the regression equations. This will be easier to code and maintain since the longwave radiation in the current model is calculated every three hours. However, if it can be afforded calculating the longwave radiation every time step or at least a shorter time duration, then a full three OLR variables could be used since it may help improve rainfall forecast beyond three days.

5. A FURTHER TEST OF THE SCHEME FOR DRY AND WET MONSOONS

The improved precipitation forecast in the monsoon regions using the outgoing longwave radiation is attributed to the better handling of the cloud and the associated moisture fields. Then a question can be raised as follows: would the outgoing longwave radiation remain a good predictor for the precipitation if the cloud fields are suppressed and become more scattered in a dry monsoon? To examine the performance of the extended cumulus parameterization and rainfall rate scheme under such an unusual weather conditions, we performed two six day forecasts starting on 1 June for 1987 and 1988. During 1987 and 1988, the monsoon seasons in most parts of the tropics experienced a dramatic swing from extreme dry to wet or vice versa. In 1986, most parts of India experienced delay in the onset of the monsoon by 4–5 days. The average rainfall for the whole India was 786 mm as compared to a climatic normal of 853 mm (between 1871–1978). During the summer of 1987, the northward

movement of the monsoon was abnormally arrested. The average rainfall for the India as a whole plummeted to 707 mm. However, in 1988, the monsoon arrived the southern India in early June and advanced northward slowly through June and July. Although the monsoon season was shorter, most of India received above–normal monsoon rain. The overall average rainfall of India was 1018 mm.

Over east China, the summer monsoons of 1986 and 1987 were persistently weaker than usual. It resulted in a large area of summer drought over central China between 33° and 40°N where rainfall over several areas was less than 50% of the normal rainfall. Unlike the previous two years, 1986 and 1987, 1988 was a strong monsoon year over east China. For the first time, most of China (particularly the north) received abundant rain in the summer. While India and eastern China received sub–normal rainfall in both 1986 and 1987, west Africa received above or near–normal rainfall between 1986 and 1988.

Again we compared the rainfall forecasts with the rainfall derived from satellite. Since the rain gauge data were not assimilated into satellite observations, we only used the areal mean rainfall as a measure of relative performance of the extended rainfall scheme. We select three sectors: India bounded by 5°N to 20°N and 75°E and 90°E, east China bounded by 20°N to 30°N and 110°E to 120°E, and west Africa bounded by 0°N to 25°N and 20°W to 0°W. These three sectors correspond to three locations that have experienced a dramatic swing in monsoon rainfall. The areal mean rainfalls for 1987 are summarized in Table 7. The values in columns 1 through 3 are the satellite derived rain fall, rainfall rate forecast with OLR variables, and rainfall rate forecast without the OLR variables. In the India sector, the areal mean rainfall from both forecasts are small compared to the same areal mean rainfall derived from satellite, which has a value of daily rainfall rate of 20 mm. Between the two forecasts, the areal mean rainfall forecasts using the OLR are even smaller, and they are consistent with the dry condition in the beginning of the 1987 monsoon season. In the East China sector, the mean areal rainfall using OLR increases from 2 mm on day 1 to 56 mm on day 4 and it drops to 31 mm on day 6. During the first three days, the values of the daily rainfall show a similar

trend in the satellite date. However, the alternate mean areal rainfall rate with excluding OLR increases from 12 mm on day 1 to 16 mm on day 2 and then it decreases to 6 mm on day 6. Over west Africa, the mean areal rainfall derived from the satellite OLR increased from 3 mm on day 1 to 8 mm on day 6. The mean areal rainfall using the OLR increased from 2 mm on day 1 to 13 mm on day 6, and they are closer to the satellite data. The mean areal rainfall excluding OLR does not show a similar progressive increase in the rainfall during the 6 days, and they depart even further from satellite data.

In 1988 (Table 8), the satellite observations for two days in June were missing. In India, both forecasts are very similar, and the values are also low in the mean areal rainfall. This is probably because the first surge of monsoon just came to the southern part of India, and the monsoon is still considered dry. The four forecasts for India in 1987 and 1988 differ little, and they are characteristically small as compared to the mean area rainfall compared to satellite. In the east China, the mean area rainfall forecasts from using OLR lie between those obtained form satellite and from excluding OLR. In west Africa, the mean area rainfall forecast with the OLR are closer to the satellite data.

6. CONCLUSION

The Kuo type cumulus parameterization and rainfall rate scheme is extended and improved by including OLR, the local time rate change of OLR, and the horizontal Laplacian of OLR. The extended scheme remains simple and efficient. A series of 5–day forecasts of 1979 monsoon for the tropical belt between the Arabian Sea and the western Pacific Ocean show an improvement in the 3–day forecast in the daily accumulated precipitation and the location. Further RMS error analyses indicate that using OLR and the horizontal Laplacian of OLR also produces a significant improvement in a three–day forecast, even though the RMS errors are slightly larger than those obtained from all three OLR variables. Additional test of this extended scheme for the 1987 and 1988 monsoons produced consistent and characteristic rainfall rates over India, east China and west Africa even when these regions experienced a

dramatic swing in monsoon rainfall amounts.

7. ACKNOWLEDGEMENTS

The authors thank Professor Steven Esbensen for providing them the A/B scale rainfall data from GATE. We also thank Kevin Ingles for this programming assistance. The work is supported by Air Force grant no. AFOSR-91–0023.

8. REFERENCES

Arakawa, A., and W. H. Schubert, 1974: Interaction of a cumulus cloud ensemble with the large–scale environment. Part I. J. Atmos. Sci., 31, 674–701.

Betts, A.K., and Miller, M.J. 1986: A new convective adjustment scheme. Part II: Single column tests using GATE, BOMEX, ATEX and Arctic air–masss data sets. Q.J.R. Meteorol. Soc. 112, 693–709.

Businger, J. A., J. C. Wyngaard, Y. Izumi, and E. F. Bradley, 1971: Flux profile relationship in the atmospheric surface layer. J. Atmos. Sci. 28, 181–189.

Davies, R.,1982. "Documentation of the Solar Radiation Parameterization in the GLAS Climate Model," NASA Tech. Memo. 83961. Goddard Space Flight Cent., Greenbelt, Marylands.

Grell, G. A., Y.–H. Kuo, and R. J. Pasch, 1991: Semiprognostic tests of cumulus parameterization schemes in the middle latitudes. Mon. Wea. Rev., 119, 5–31.

Harshvardhan, and T. G. Corsetti, 1984: Longwave parameterization for the UCLA/GLAS GCM. NASA Tech. MEM. 85072, Goddard Space Flight Center, Greenbelt, MD.

Harshvardhan, R. Davis, D. A. Randall, and T. G. Corsetti, 1987: A fast radiation parameterization for atmospheric circulation models. J. Geophy. Res., 92, 1009–1016.

Janowiak, J. E., and P. A. Arkin, 1991: Rainfall variations in the tropics during 1986–1989, as estimated from observations of cloud–top temperature. J. Geophys. Res., 96, 3359–3373.

Krishnamurti, T. N., S. Low–Nam ,and R. Pasch, 1983a: Cumulus parameterization and rainfall rates II. Mon. Wea. Rev., 111, 815–828.

Krishnamurti, T. N., S. Cocke, R. Pasch and S. Low–Nam, 1983b: Precipitation estimates from rain gauge and satellite observations summer MONEX. Rep. No. 83–7, Dept. of Meteorology, Florida State University (avail. from Dept. of Meteor., Florida State University, Tallahassee, FL. 32306).

Krishnamurti, T. N., and H. S. Bedi, 1988: Cumulus parameterization and rainfall rates: Part III. Mon. Wea. Rev., 116, 583–599.

Krishnamurti, T. N., A. Kumar, K. S. Yap, A.P. Dastoor, N. Davidson, and J. Sheng, 1990: Advances Geophys., R. Dmowska and B. Saltzman, eds., Academics Press, Vol. 33, 133–281.

Kuo, H. L., 1974: Further studies of parameterization of parameterization of the influence of cumulus convection on large scale flow. J. Atmos. Sci., 31, 1232–124.

Louis, Jean–Francois, 1979: A parametric model of vertical eddy fluxes in the atmosphere. Bound. Layer Meteor., 17, 187–202.

MacVean, M. K., 1983: The effects of horizontal diffusion on baroclinic development in a spectral model. Quart. J. Roy. Meteor. Soc., 109, 771–789.

Tiedtke, M., 1989: Cumulus parameterization: thermodynamic aspects. Ten Years of Medium–Range Weather Forecasting. Vol. II, pp 39–66. ECMWF World Meteorological Organization, 1990: The global climate system: June, 1986–November 1988.

Wu, Man–LI, C., 1991: Global precipitation estimates from satellite using difference fields of outgoing long–wave radiation. Atmos. Ocean., 29, 150–174.

Table 1 the coefficients of multiple regime equation
for (1) including all three OCR variables and
for (2) excluding OCR variables.

	(1)		(2)	
	R/I	M/I	R/I	M/I
C_o	1.025	–6.001	1.294	0.3037
C_1	0.323×10^4	-0.681×10^5	0.8637×10^4	-0.3818×10^5
C_2	0.1865×10^3	-0.5196×10^3	0.3771×10^3	0.9207×10^3
C_3	0.0193	1.631		
C_4	0.1033×10^5	0.6736×10^4		
C_5	0.1292×10^{11}	0.6261×10^{11}		

Table 2. Root mean square errors for the new forecasts including all three OCR variables

		Accumulated Rainfall	Location
	day 1	21.8	0.45
India sector	day 2	18.6	0.49
	day 3	14.4	0.54
ON–22N	day 4	28.1	0.60
62E – 80E	day 5	32.0	0.70
	day 1	17.6	0.61
Burma Sector	day 2	31.0	0.57
0N – 20N	day 3	27.0	0.54
95E – 110E	day 4	35.1	0.57
	day 5	27.8	0.69
Western Pacific	day 1		0.62
0N – 22N	day 2		0.58
110E – 150Ed	day 3		0.54
	day 4		0.63
	day 5		0.72

Table 3. Root mean square errors for the control forecast excluding OLR variables

		Accumulated Rainfall	Location
	day 1	24.7	0.49
India sector	day 2	25.5	0.60
	day 3	18.7	0.68
ON–22N	day 4	25.6	0.67
62E – 80E	day 5	18.9	0.60
Burma sector	day 1	17.6	0.58
0N–20N	day 2	19.3	0.59
95E – 110E	day 3	28.7	0.59
	day 4	22.9	0.55
	day 5	16.0	0.56
Western Pacific	day 1		0.71
	day 2		0.70
0N–22N	day 3		0.70
110E–150E	day 4		0.73
	day 5		0.70

Table 4 Root mean squares error for the new cast with OLR variability

		Accumulated Rainfall	Location
India Sector	day 1	21.1	0.44
	day 2	28.0	0.56
	day 3	40.7	0.70
ON–22N	day 4	40.8	0.78
62E – 80E	day 5	25.0	0.73
Burma sector	day 1	18.6	0.58
0N–20N	day 2	24.9	0.57
95E – 110E	day 3	36.4	0.58
	day 4	35.1	0.62
	day 5	21.7	0.62
Western Pacific	day 1		0.63
	day 2		0.60
0N–22N	day 3		0.61
110E–150E	day 4		0.65
	day 5		0.73

Table 5. Root mean square errors from the new forecast including OLR and the local time rate change of OLR

		Accumulated Rainfall	Location
India Sector	day 1	20.0	0.42
	day 2	30.1	0.57
	day 3	43.4	0.73
ON–22N	day 4	41.9	0.78
62E – 80E	day 5	26.6	0.73
Burma sector	day 1	18.6	0.57
0N–20N	day 2	22.0	0.54
95E – 110E	day 3	45.0	0.57
	day 4	38.7	0.59
	day 5	23.8	0.63
Western Pacific	day 1		0.63
	day 2		0.60
0N–22N	day 3		0.63
110E–150E	day 4		0.68
	day 5		0.75

Table 6. Root mean square error from the new forecast including OLR and the Laplacian of OLR

		Accumulated Rainfall	Location
	day 1	21.4	0.44
India sector	day 2	18.9	0.48
	day 3	17.8	0.59
0N–22N	day 4	33.0	0.66
62E – 80E	day 5	28.54	0.65
Burma sector	day 1	17.9	0.59
0N–20N	day 2	30.2	0.56
95E – 110E	day 3	39.6	0.51
	day 4	39.6	0.55
	day 5	29.9	0.65
Western Pacific	day 1		0.61
	day 2		0.60
0N–22N	day 3		0.58
110E–150E	day 4		0.58
	day 5		0.70

Table 7. A real mean rainfall for 1987 obtained from (1) satellite data, (2) a forecast including all three OLR variables, (3) a forecast excluding all three OLR variables

		1	2	3
	day 1	23.2	2.7	3.7
India sector	day 2	23.4	3.4	5.5
	day 3	23.7	2.2	4.0
5N–20N	day 4	20.0	4.6	8.7
75E–90E	day 5	18.3	4.2	5.9
	day 6	17.6	5.6	4.7
East China	day 1	10.2	7.2	11.6
20N–30W	day 2	15.4	11.7	15.7
110E–120E	day 3	16.0	17.1	10.5
	day 4	18.5	56.1	5.3
	day 5	20.3	36.5	4.3
	day 6	21.2	31.2	6.5
West Africa	day 1	2.6	1.91	2.2
	day 2	4.5	5.2	6.2
	day 3	4.9	4.3	3.8
0N–25N	day 4	6.9	6.8	6.6
20W–0W	day 5	7.7	11.3	6.1
	day 6	8.3	13.6	5.6

Table 8. A real mean rainfall for 1988 obtained from (1) satellite data, (2) a forecast including all three OLR variables, (3) a forecast excluding all three OLR variables

		1	2	3
	day 1	–	5.0	7.8
India sector	day 2	–	6.1	13.0
	day 3	14.9	4.5	4.5
5N–20N	day 4	13.0	6.8	4.2
75E–90E	day 5	14.0	6.2	8.0
	day 6	17.3	6.2	5.8
East China	day 1	–	10.6	16.0
	day 2	–	15.4	18.6
	day 3	5.9	27.8	26.1
20N–30N	day 4	1.22	12.0	22.4
110E–120E	day 5	2.17	9.6	19.7
	day 6	3.3	6.9	8.68
West Africa	day 1	–	1.6	1.4
	day 2	–	3.3	2.4
	day 3	7.4	7.7	2.8
0N–25N	day 4	7.3	7.5	4.6
20W–0W	day 5	7.5	6.5	3.8
	day 6	7.6	1.3	3.5

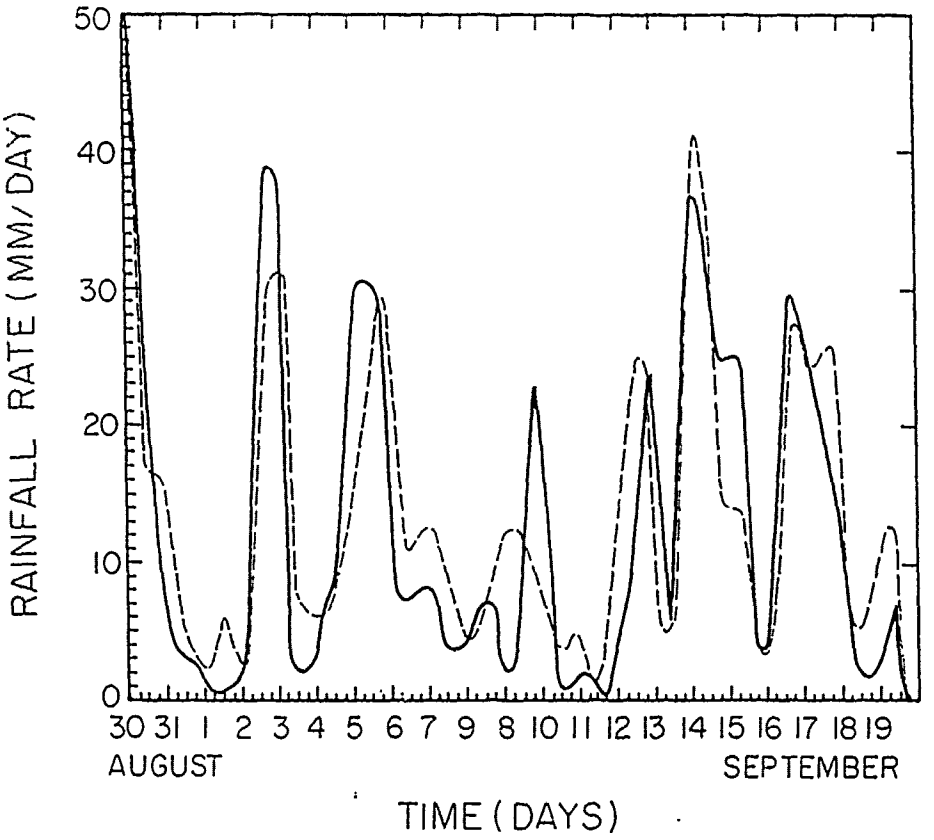
RAINFALL RATE (MM/DAY)
50
40
30
20
10
0
30 31 1 2 3 4 5 6 7 9 8 10 11 12 13 14 15 16 17 18 19
AUGUST
SEPTEMBER
TIME (DAYS)

a

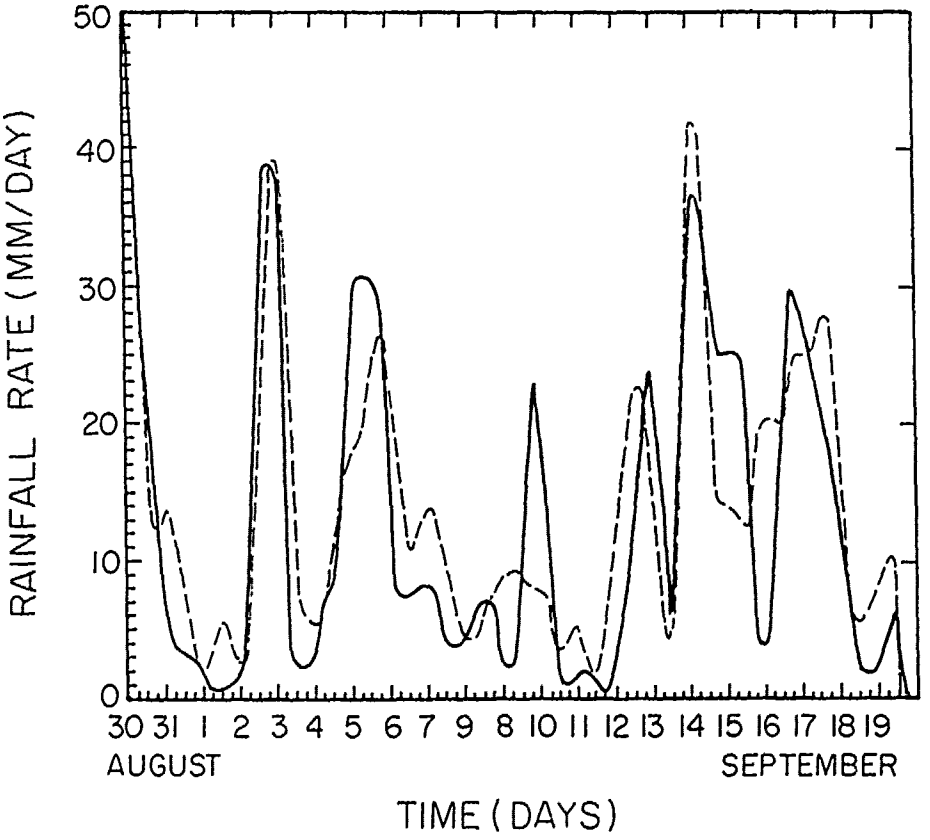
RAINFALL RATE (MM/DAY)
50
40
30
20
10
0
30 31 1 2 3 4 5 6 7 9 8 10 11 12 13 14 15 16 17 18 19
AUGUST
SEPTEMBER
TIME (DAYS)

b

1a & b

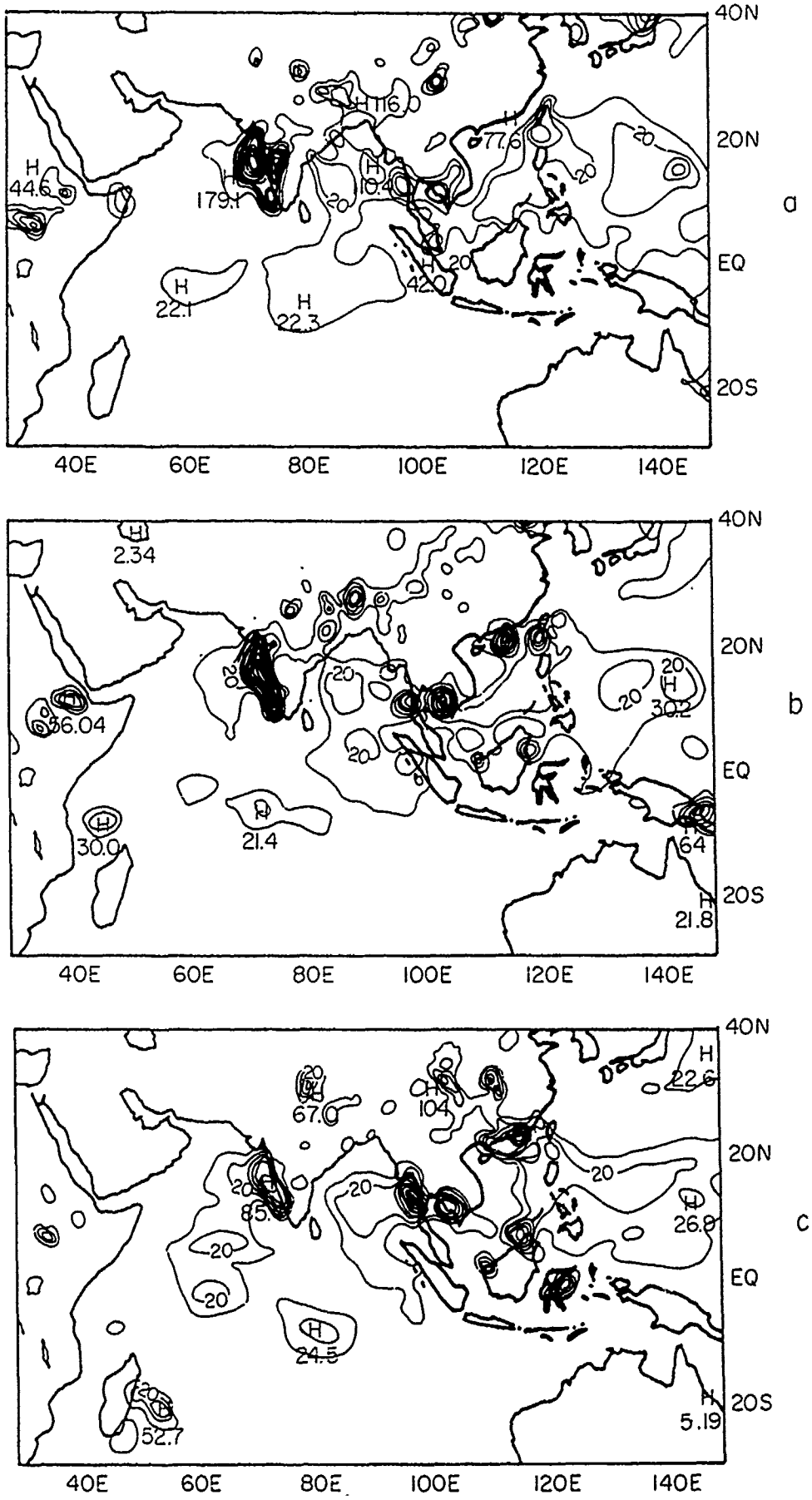
40N
20N
EQ
20S
40E
60E
80E
100E
120E
140E
a
H
44.6
179.1
116.0
77.6
10.4
42.0
22.1
22.3
20
b
2.34
36.04
30.0
21.4
30.2
64
21.8
c
67.0
104
22.6
85.
26.8
24.5
52.7
5.19

2a,b&c

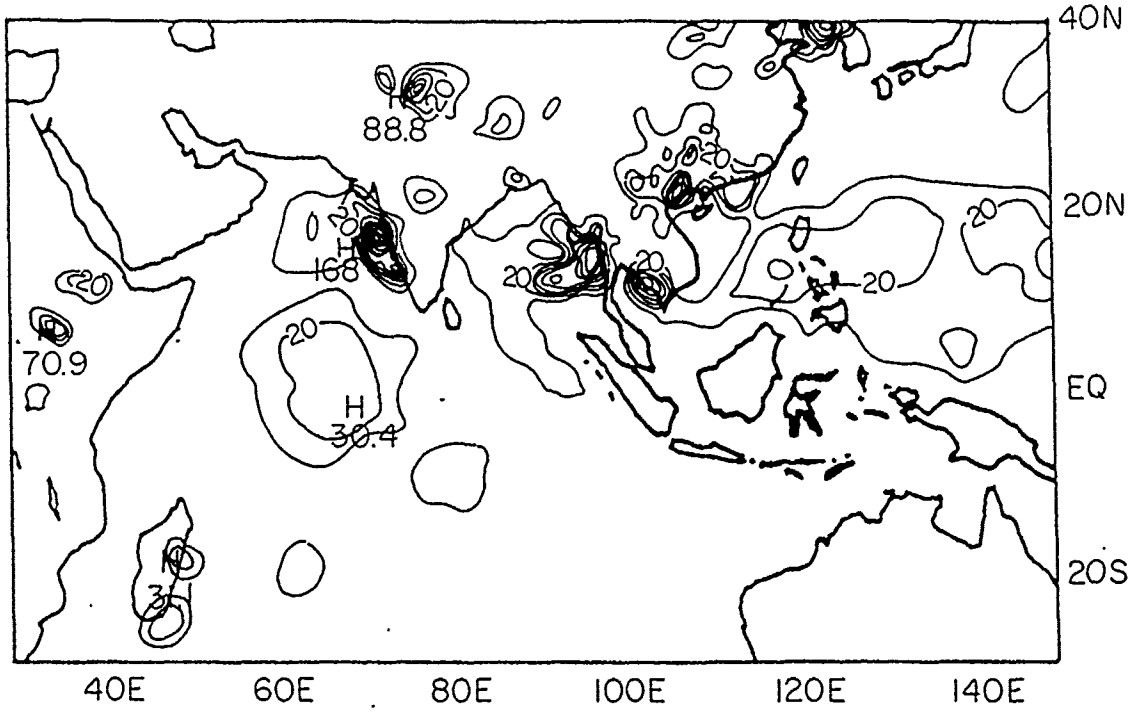
40N
20N
EQ
20S
40E
60E
80E
100E
120E
140E
88.8
168
70.9
30.4
20
d

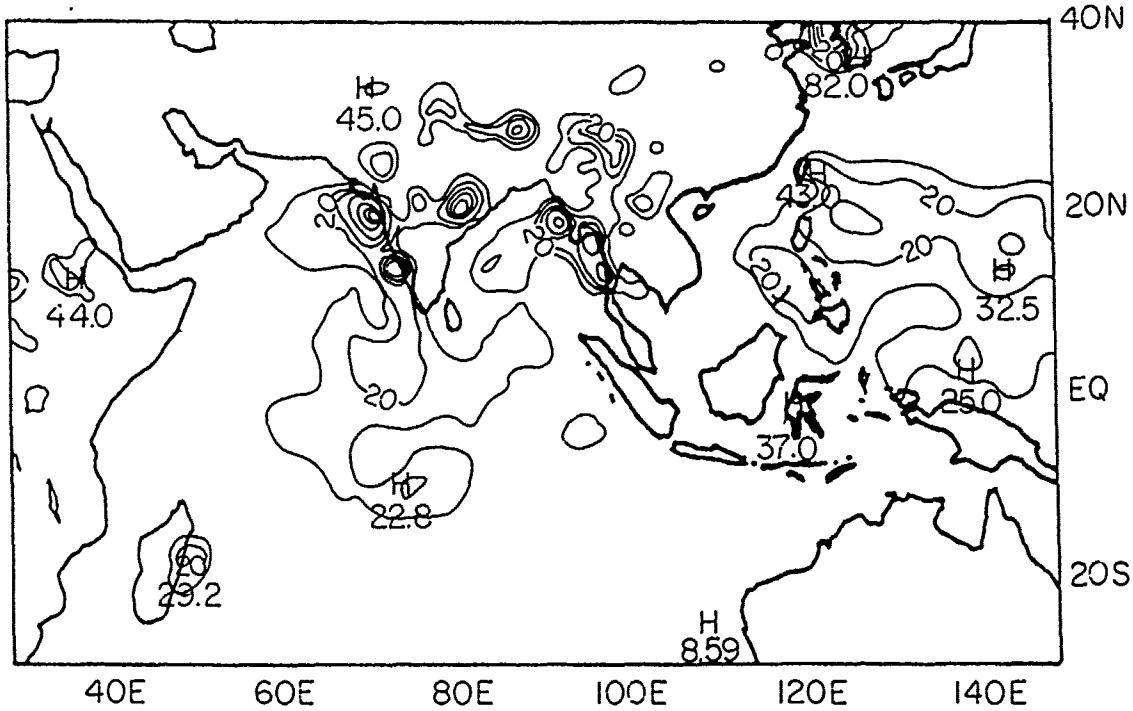
40N
20N
EQ
20S
40E
60E
80E
100E
120E
140E
45.0
82.0
44.0
32.5
25.0
37.0
22.8
23.2
8.59
20
e

2d&e

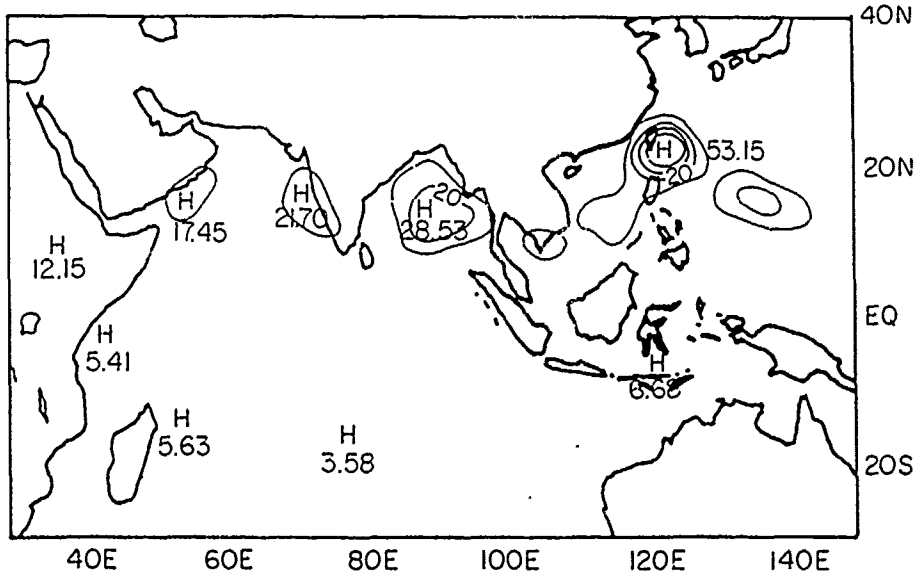
40N
20N
EQ
20S
40E
60E
80E
100E
120E
140E
H 53.15
20
H 17.45
H 21.70
H 28.53
H 12.15
H 5.41
H 6.68
H 5.63
H 3.58

a

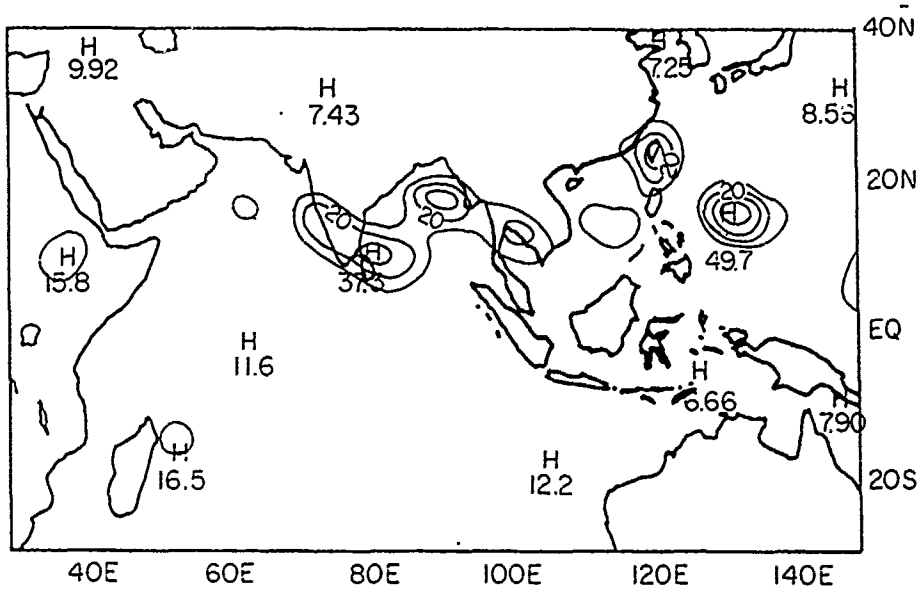
40N
20N
EQ
20S
40E
60E
80E
100E
120E
140E
H 9.92
H 7.43
H 7.25
H 8.56
20
H 49.7
H 15.8
H 37.3
H 11.6
H 6.66
H 7.90
H 16.5
H 12.2

b

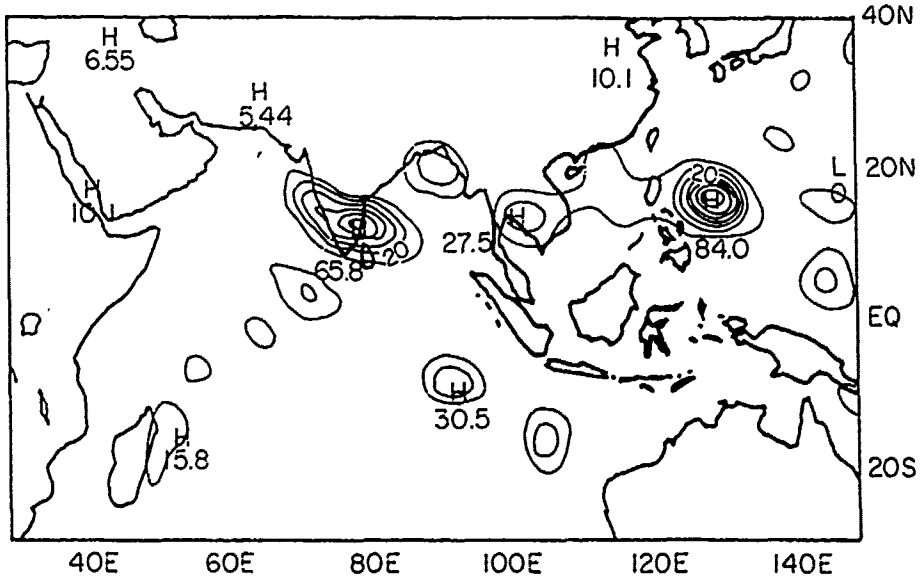
40N
20N
EQ
20S
40E
60E
80E
100E
120E
140E
H 6.55
H 5.44
H 10.1
L
20
H 84.0
H 27.5
65.8
H 30.5
H 5.8

c

3a,b&c

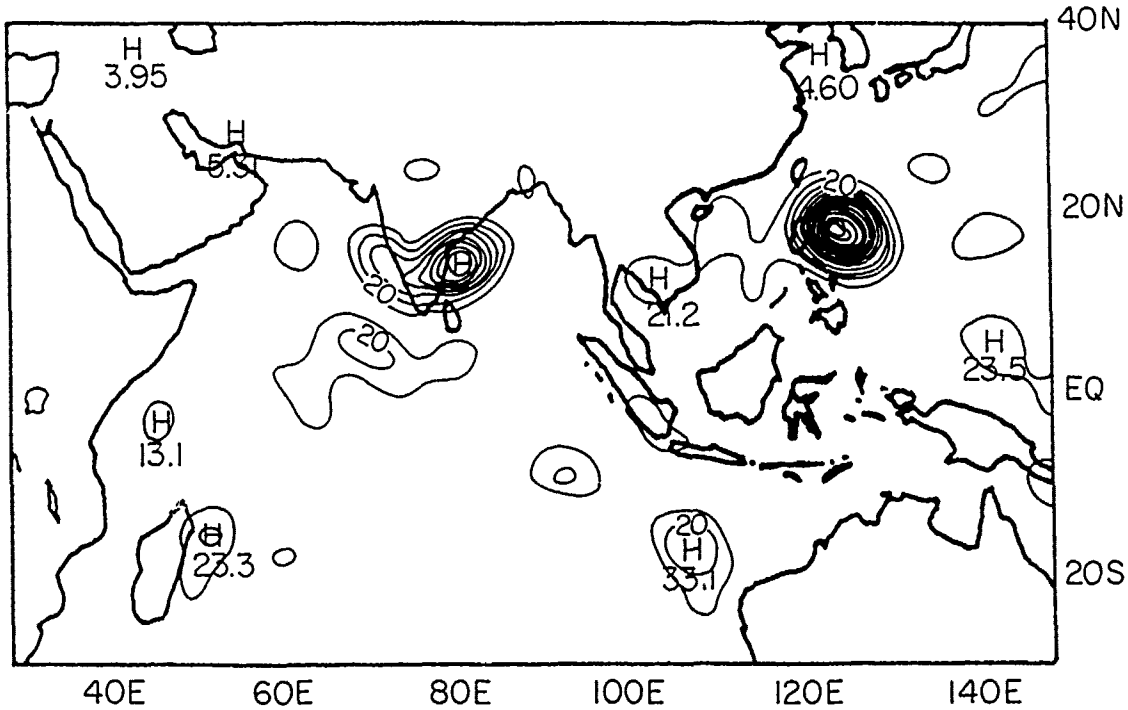
40N
20N
EQ
20S
40E
60E
80E
100E
120E
140E
H
3.95
H
4.60
H
5.31
20
H
21.2
H
23.5
H
13.1
H
23.3
20
H
33.1

d

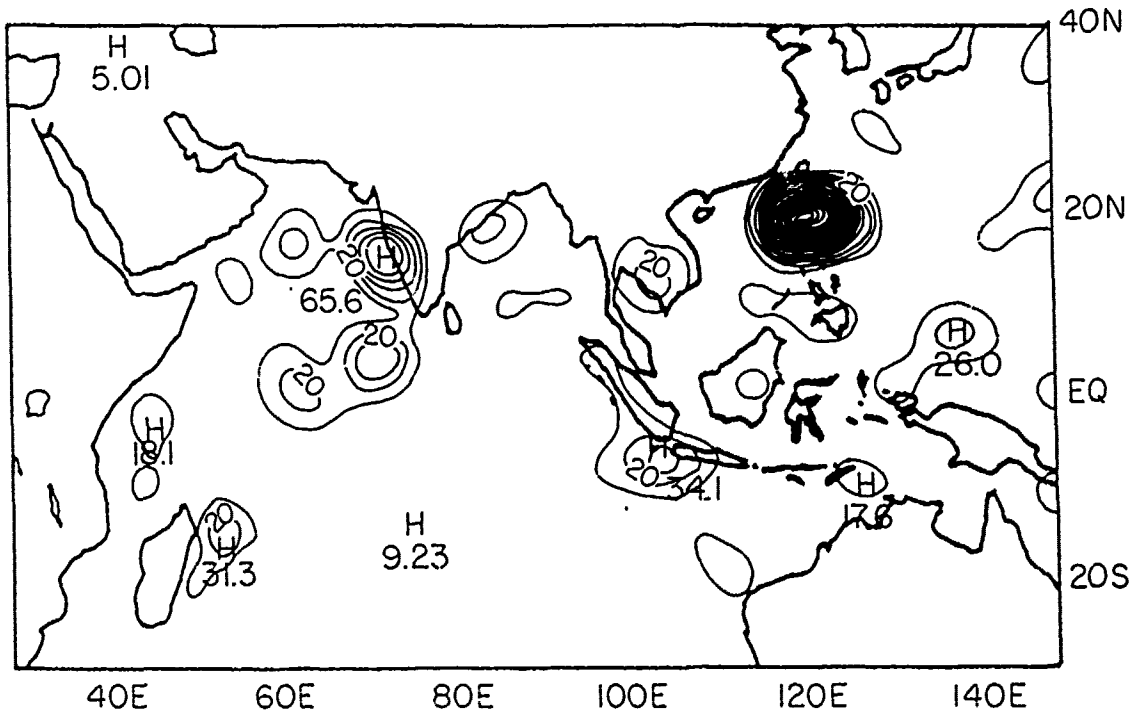
40N
20N
EQ
20S
40E
60E
80E
100E
120E
140E
H
5.01
H
65.6
20
H
26.0
H
18.1
20
H
31.3
H
9.23
H
34.1
H
17.6

e

3d & e

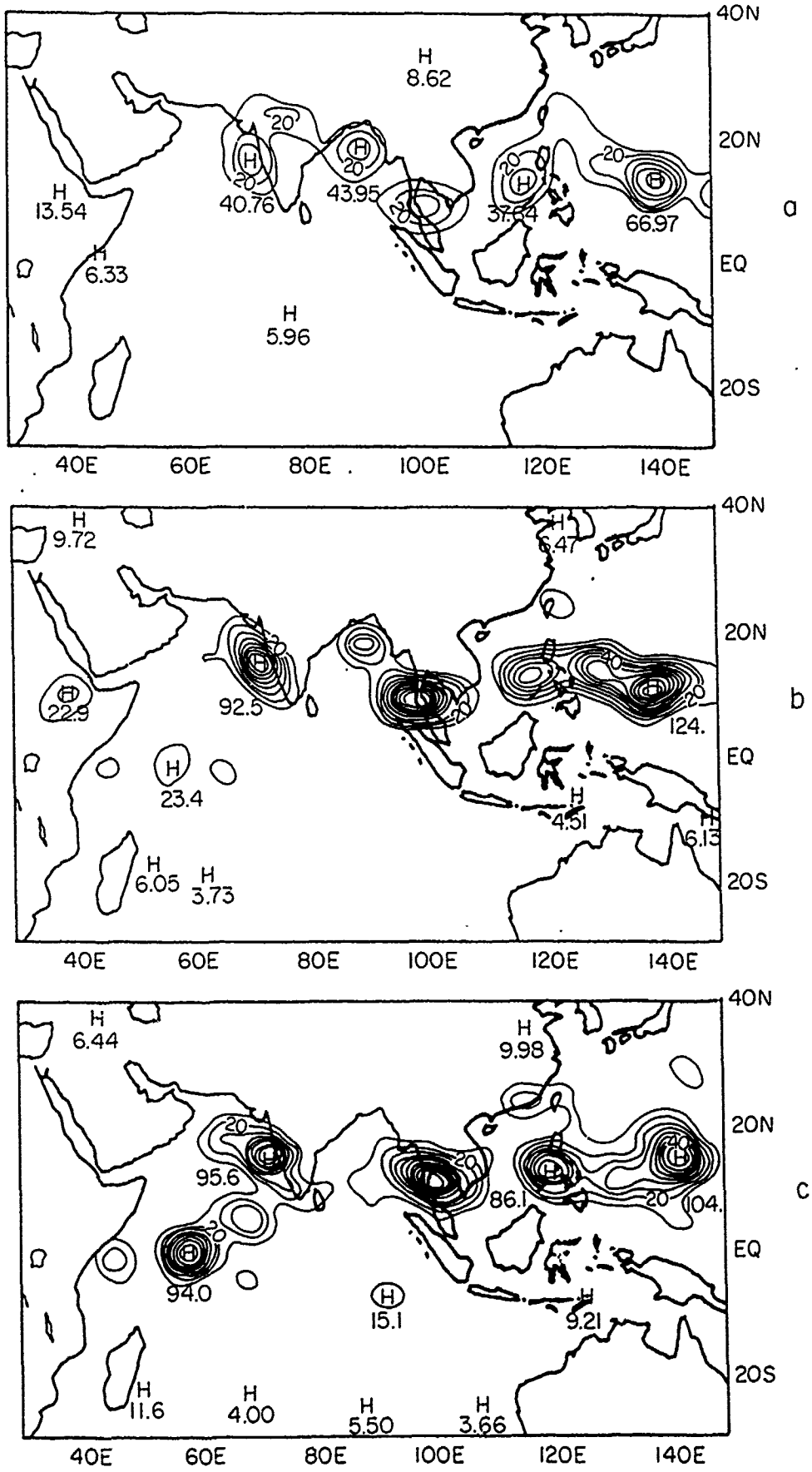
40N
20N
EQ
20S
40E
60E
80E
100E
120E
140E
a
H 8.62
H 13.54
H 6.33
H 5.96
40.76
43.95
37.64
66.97
b
H 9.72
H 6.47
22.9
92.5
124.
23.4
4.51
6.13
6.05
3.73
c
H 6.44
H 9.98
95.6
86.1
104.
94.0
15.1
9.21
11.6
4.00
5.50
3.66

4a,b & c

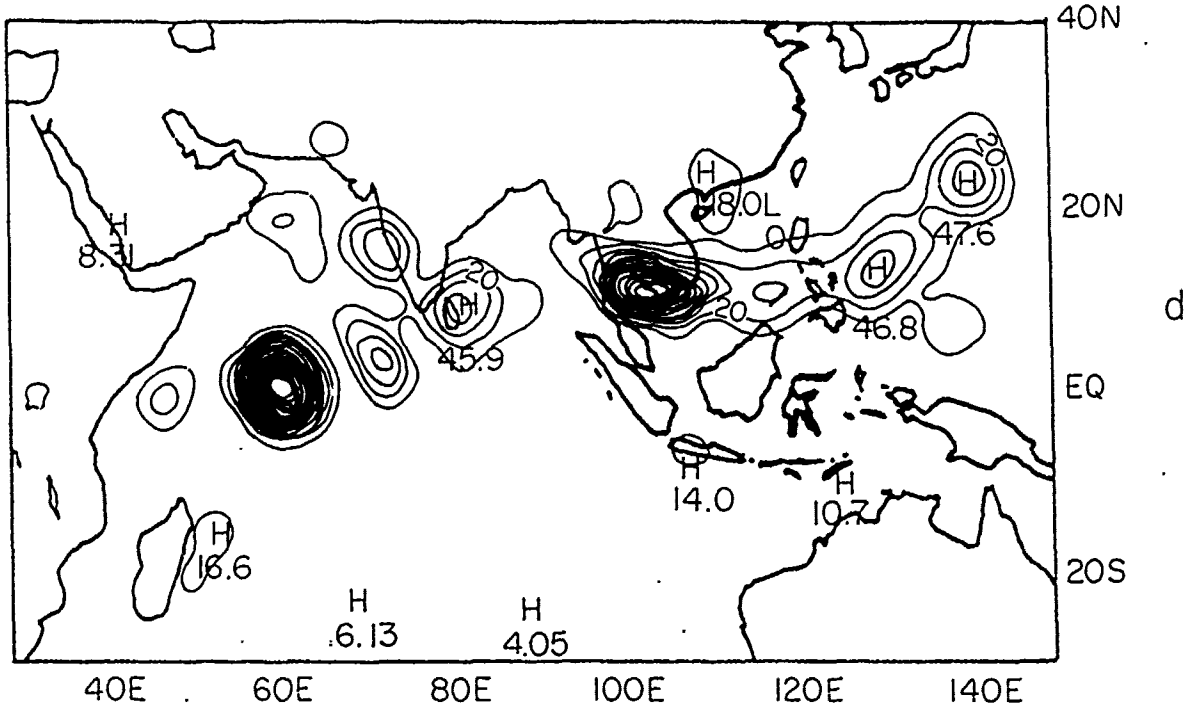
40N
20N
EQ
20S
40E
60E
80E
100E
120E
140E
d
H
8.31
H
18.0L
H
47.6
H
46.8
H
45.9
H
14.0
H
10.7
H
16.6
H
6.13
H
4.05

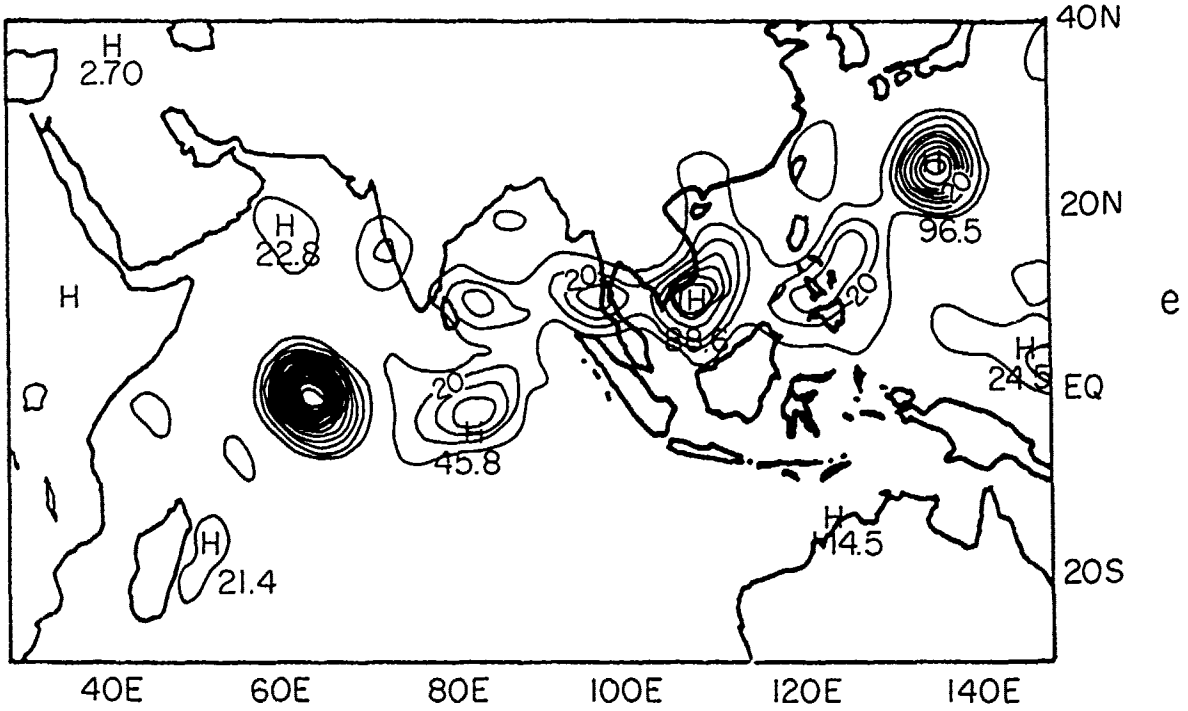
40N
20N
EQ
20S
40E
60E
80E
100E
120E
140E
e
H
2.70
H
22.8
H
96.5
H
39.6
H
24.5
H
45.8
H
14.5
H
21.4

4d & e